World Academy of Science, Engineering and Technology
International Journal of Aerospace and Mechanical Engineering
Vol:1, No:4, 2007

Development of Blower for Air Management System of Fuel Cell Modules

Joo-Han Kim, Jung-Moo Seo, Ha Gyeong Sung, and Se Hyun Rhyu

***Abstract*—**This study presents a blower for air management system of fuel cell modules. A blower is composed of BLDC motor and impeller. Magnetic equivalent circuit model and finite element analysis are used to design the motor, and an improved structure is considered to reduce a mechanical loss induced from bearing units. Finally, air blower system combined with the motor and an impeller is manufactured and output properties, such as an air pressure and an amount of flowing air, are measured. Through the experimental results, a validity of the simulated one is confirmed.

***Keywords*—**Fuel cell modules, BLDC motor, Impeller, Air management.

I. Introduction

RECENTLY, due to the exhaustion of fossil fuel, pollution of air, and demand for capacity increase of power system, new generating technologies using various energy sources, for instance wind, water, geothermal, fuel cell, have been developed. Among them, fuel cell system which generates electric energy from chemical reaction of hydrogen and oxygen is considered one of the promising alternatives due to aspects of environment conservation as well as high efficiency [1, 2]. Fuel cell systems consist of fuel cell stack, air management system, and power conditioning system. Air management systems composed of pump, fan, compressor, and blower determine output performance of overall system on the preferential basis. Besides, the proper matching of a motor's speed/torque curve to aerodynamic output is especially important in increasing efficiency thereby reducing its demand on a fuel cell system. Several advantages of the brushless motor compared to DC motor could meet the above goal and spark-free characteristic is essential factor considering a flammable hydrogen gas produced in proton exchange membrane units.

This paper deals with a design of the air management system, especially BLDC motor for the blower module. Designed motor is manufactured and assembled into the blower, and then the simulated results are verified by the experimental one.

II. BLDC Motor Design and Simulation

In this paper, we have used the 2D Finite Element Method for calculating the characteristics of BLDC Motor. The governing equation of 2D FE analysis model is equation (1).

Authors are with Korea Electronics Technology Institute, 203-101 B/D 192, Yakdae-dong, Wonmi-gu Gyeonggi-do, Korea (phone: +82 / (32) – 621.2852; fax: +82 / (32) – 621.2855; e-mail: kimjh@keti.re.kr).

$$\frac{1}{\mu}\left(\frac{\partial^2 A_z}{\partial x^2}+\frac{\partial^2 A_z}{\partial y^2}\right)=-J-\frac{1}{\mu_r}\left(\frac{\partial M_{ry}}{\partial x}+\frac{\partial M_{rx}}{\partial y}\right) \quad (1)$$

Here, A is magnetic vector potential and J is current density of coil. If the analysis model is infinite to z axis direction, **A** and J are existed only to z axis direction. Also, M_r is residual magnetization.

In order to determine the output characteristics of the motor, input characteristics of the combined impeller system are needed. From the simulated results of the impeller system, required rotational speed and torque at rated load are fixed up. Apart from the rated operations, a blower module is needed to work under maximum speed often. Due to the water formed on a membrane caused by hydrogen protons and oxygen, more output power is necessary. Table I shows the required specification of the motor. Based on the specification, first of all, rough design is conducted using magnetic equivalent circuit model [3]. Table II presents the designed parameters of the motor. In order to have advantage in a constant high rotation speed and cool down a heat generated from operation of long duration, we selected exterior rotor type BLDC motor.

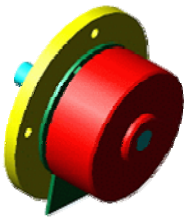

Fig. 1 BLDC motor CAD

TABLE I
THE REQUIRED SPECIFICATION OF MOTOR

Items		Specifications
Motor	Input voltage [V]	24
	Rated load [mNm]	45
	Rated speed [rpm]	11,000
	Maximum load (duty 100%) [mNm]	65
	Maximum speed (duty 100%) [rpm]	14,500
	Outer diameter [mm]	≤ 60
	Efficiency [%]	≥ 70
Blower system	Rated air pressure [kPa]	15
	Rated air flow [LPM]	70
	Maximum air pressure [kPa]	25
	Maximum air flow [LPM]	100

TABLE II
THE DESIGNED PARAMETERS OF MOTOR

Items	Design variables
Motor type	6p / 9s outer rotor BLDC
Driving type	3 Phase 2 excited
Magnet	ND-Bonded (Br = 0.6T)
Magnet thickness [mm]	2
Outer diameter of rotor [mm]	54
Laminated stator height [mm]	12
Air gap [mm]	0.5

Through a finite element analysis, performance of the designed motor is checked out and specific configurations are determined. The magnetic density distribution of the motor is expressed in Fig. 1. As can be seen in the figure, some of the rotor parts are saturated; however, considering the three dimensional structure of the rotor housing, the magnetic density of the rotor would be dispersed and decreased.

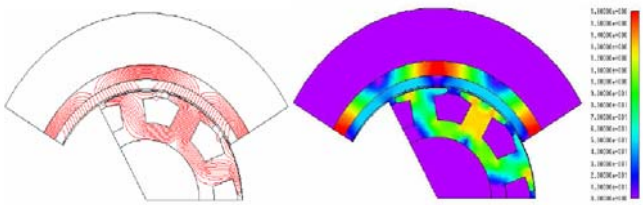

Fig. 2 Flux line and density distribution

Fig. 2 shows an induced electromotive force (EMF) and a cogging torque of the proposed motor. EMF of 15.5V0-peak is obtained at 10,000rpm, which means the required rotational speed could be generated at input voltage of 24V. Also, a torque constant calculated from the back EMF characteristic is estimated about 14mNm/A, which could be converted a generated torque of 55mNm at rated current of 4A. The calculated cogging torque, 6mNm0-peak, is about 10% of the rated torque. With the above results, we conformed the designed motor is enough to satisfy the electromagnetic needs.

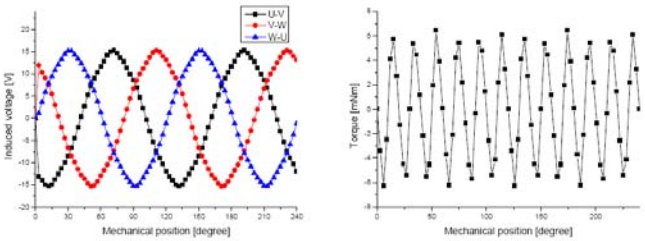

(a) Back EMFline to line @ 10,000rpm (b) cogging torque
Fig. 2 Calculated back EMF waveform and cogging torque

III. EXPERIMENT AND DISCUSSION OF BLDC MOTOR

Manufactured trial product is shown in Fig. 3. A pair of bearings is placed in up and down space of a base yoke, and wave washer is put in the bottom of the one bearing. Hall PCB for sensing a rotational position is assembled under a stator core. Fig. 4 shows experimental results of induced EMF at 1,000rpm and switching current of the motor. Advance switching current angle of 15 degree is set not to have a condition of current waveform distort for reduction of torque ripple and vibration.

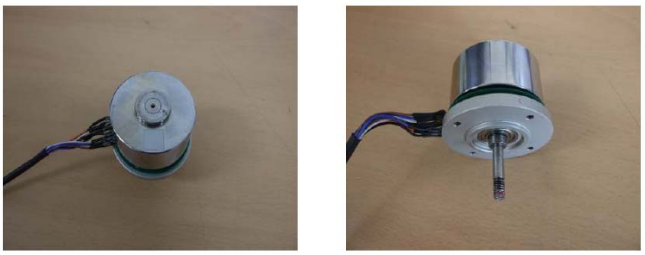

Fig. 3 Manufactured motor

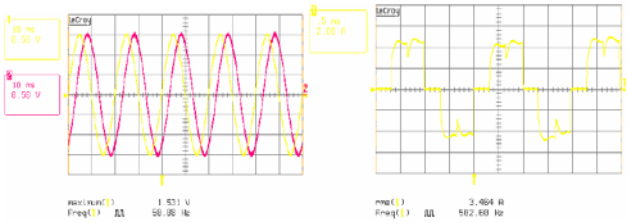

(a) Back EMFline to line @ 1,000rpm (b) Current waveform @ 10,000rpm
Fig. 4 EMF and current measurement

In order to measure the characteristics of the designed motor, commercial torque detectors (EMA-1,SUGAWARA) are used. As a result of test, however, rotational speed of the motor is decreased and the input current is increased as compared with a simulated one. Consequently, the efficient of the motor is declined a little. Many-sided tests and analyses let us come to a conclusion that the performance drop is originated from restriction condition of the motor assembling. When the motor is coupled with impeller of a blower, to avoid the shaking of the impeller in the direction of a rotational axis, the shaft of the

motor combined the impeller's center should be restricted in axial direction. Especially, in the case of very small gap is required between impeller and housing of blower, small swing on operating could cause a fatal mechanical damage. In this study, the air gap of the impeller is about 80μm, so elastic force of the wave washer takes a role of preventing axial directional vibration. With those conditions, bearing's inner part tightens a fixing ring and that causes increase of mechanical loss. Besides, to guarantee a stable connection an impeller with the motor, a thick shaft of the motor is required to some extent. At a high speed, the thick shaft would make wider surface area contacting the inside of bearings; it could cause a increasing friction loss. Therefore, a narrow manufacturing tolerance between the shaft and the inside diameter of bearings is required. Shrink-fit assembly between the shaft and rotor yoke is adapted at first; however, it is not easy to overcome a eccentricity induced from cohesion process. In order to solve the mentioned problems, we put a flat washer made by a Teflon material on the upper bearing instead of the wave washer, which could reduce the friction loss between the bearing and the shaft. Also, we manufactured the shaft and the rotor yoke separately. It means that the precise abrasion processed shaft is put the bearings decreasing a mechanical manufacturing tolerance and rotor yoke is united with the top of the shaft. Fig. 5 shows the inside part and the assembly process of the motor. The characteristics of the improved motor are shown in Fig. 6. At a rated load, rotational speed of 10,800rpm, output power of 52W, and efficiency of 73% are measured, also maximum load characteristics of 14,800rpm, 102W, 75% are obtained at input voltage of 24V. With those results, the validity of BLDC motor design for the air blower module related with an object of this study is verified.

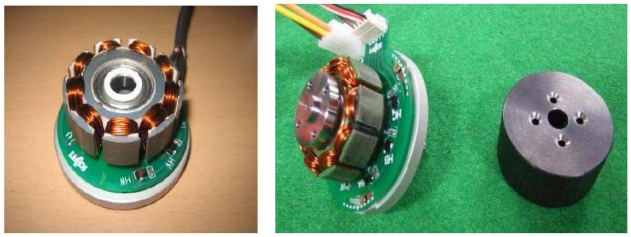

Fig. 5 Revised structure for high efficiency

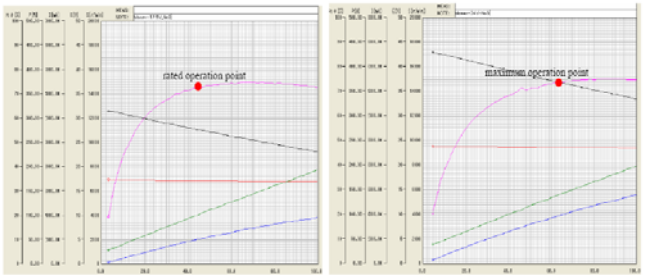

Fig. 6 Experiment result of the motor

IV. CFD Analysys of Impeller

We achieved CFD (Computational Fluid Dynamics) analysis of impeller. We used I-DEAS software to draw 3D CAD modeling and finite element modeling. We used CFX-10 software to flow analysis.

We created mesh of 3D CAD modeling by using I-DEAS Master FEM. The result is same below Fig. 7 and element and node were created as follows.

Fig. 7 CFD modeling of impeller

. Element generation: ICEM CFD 10
. Number of total element: 1,420,000
. Element type: Fan shape triangular pyramid

The boundary condition defined as following. Impeller entrance is atmospheric pressure, and impeller outlet defined as static pressure and with impeller channel interval is frozen rotor

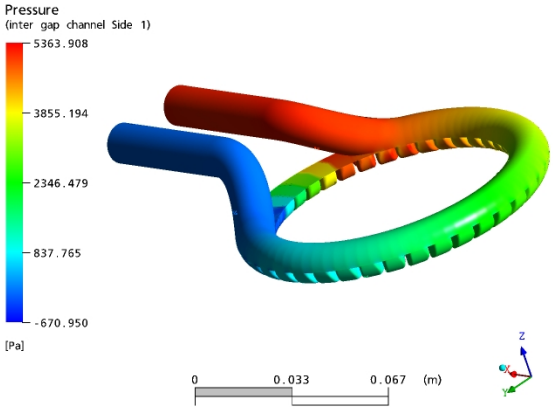

Fig. 8 CFD analysis results of Pressure distribution

Fig. 8 is CFD analysis results of impeller pressure distribution.

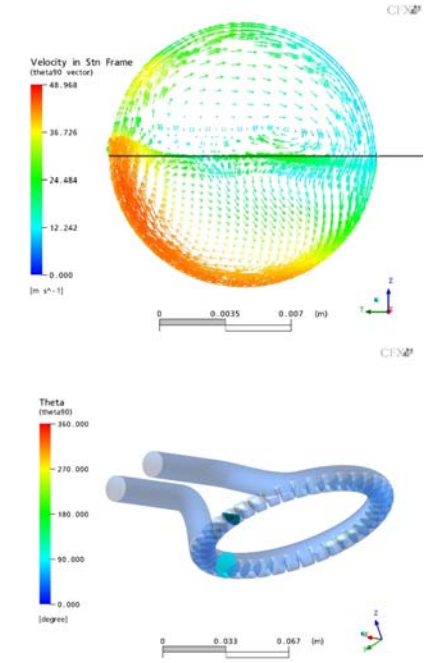

CFD analysis results of velocity distribution
(θ=90 degree)

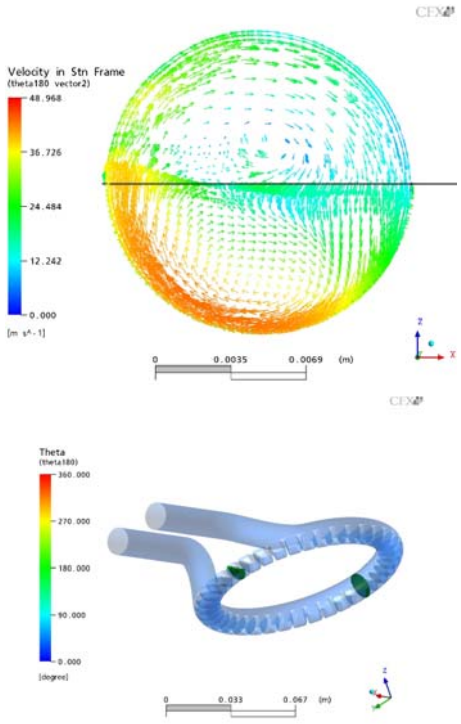

CFD analysis results of velocity distribution
(θ=90 degree)

Fig. 9 CFD analysis results of impeller velocity distribution

Fig. 9 is CFD analysis results of impeller velocity distribution

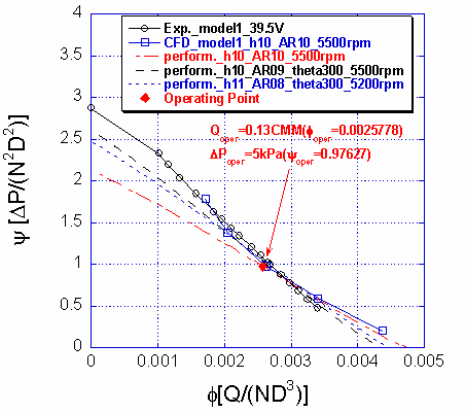

Fig. 10 CFD analysis results of static pressure

Fig. 10 is CFD analysis results of impeller static pressure.

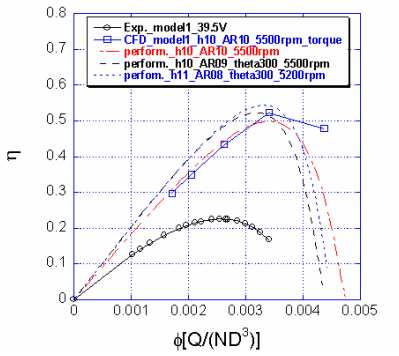

Fig. 11 CFD analysis results of efficiency

Fig. 11 is CFD analysis results of impeller efficiency.

V. Blower Characteristics Measurement

Finally, the designed motor is connected with an impeller, and output characteristics of the overall blower system with respect to pressure and flow condition changes are measured in Fig. 12 and 13. As can be seen in Fig. 8, the required output value of system, air pressure of 15kPa and air flow of 70LPM, is gained at an input voltage of 16V. Also when 24V is applied to the motor, the output characteristics of the system show good agreement with the maximum target values, such as 25kPa and 100LPM.

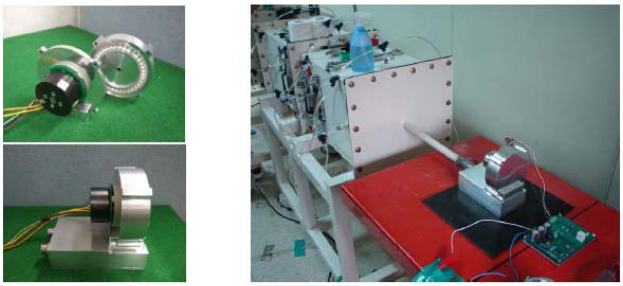

Fig. 12 Assembly of the blower module and output characteristics measurement

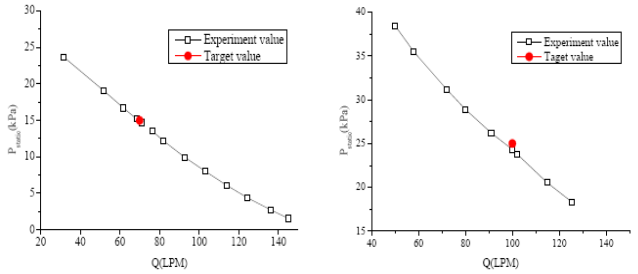

(a) 16V (rated operation condition) (b) 24V (maximum operation condition)

Fig. 13 Air pressure and flow value of the blower system in the cases of the input voltage of 16V and 24V are applied to the motor, respectively

VI. Conclusion

This study presents a design of blower module for an air management system of a fuel cell module. The motor is designed by using magnetic equivalent circuit model and finite element analysis, experimental results of the manufactured motor is compared with the simulated one. In the process, the mechanical loss is induced due to a shaft restriction in axial direction with high speed rotation. After changing mechanical assembly of the previous model, revised motor is combined with an impeller. And we achieved CFD (Computational Fluid Dynamics) analysis of impeller. Finally, output characteristics of the blower system are measured and a validity of the designed motor is confirmed.

References

[1] N. Kato and K. Kurozumi, "Hybrid power supply system composed of photovoltaic and fuel-cell systems," in Proc. INTELEC'01, Oct. 2001, pp. 631–635.

[2] M. N. Eskander and T. F. El-Shatter, "Energy flow and management of a hybrid wind/PV/fuel cell generation system," in Proc. IEEE PESC'02, Jun. 2002, pp. 347–353.

[3] J. Hur, S. B. Yoon, D. Y. Hwang and D. S. Hyun, "Analysis of PMLSM using 3 dimensional equivalent magnetic circuit network method," IEEE Trans on Mugnetics, vol 33, No. 5 pp. 4143-4145.